HHS Public Access

Author manuscript

Mol Cancer Ther. Author manuscript; available in PMC 2020 January 13.

Published in final edited form as:

Mol Cancer Ther. 2012 July ; 11(7): 1400–1410. doi:10.1158/1535-7163.MCT-12-0172.

Human Monoclonal Antibodies Targeting Nonoverlapping Epitopes on Insulin-like Growth Factor II as a Novel Type of Candidate Cancer Therapeutics

Weizao Chen, **Yang Feng**, **Qi Zhao**, **Zhongyu Zhu**, **Dimiter S. Dimitrov**

Protein Interactions Group, Frederick National Laboratory for Cancer Research, National Cancer Institute, NIH, Frederick, Maryland

Abstract

Soluble ligands are important targets for therapy of cancers and other diseases. Therapeutic monoclonal antibodies (mAb) against such ligands block their interactions with corresponding receptors but do not enhance their removal from the circulation and can increase their half-lives because of the long half-lives of the antibodies. We have hypothesized that mAbs targeting two or more nonoverlapping epitopes on the same ligand could form oligomeric antibody–ligand complexes that can bind to cells expressing Fc gamma receptors (FcγRs) with high avidity leading to their fast and irreversible removal from the circulation. Insulin-like growth factor II (IGF-II) is an example of such ligands and an important target for human cancer therapy. We identified two mAbs, m610.27 and m630.3, which bound to nonoverlapping epitopes on IGF-II with nanomolar affinity, and generated a bispecific antibody, m660. m660 inhibited the interaction of human IGF-II (hIGF-II) with the human breast cancer cell line MCF-7, hIGF-II–mediated IGF receptor type I and insulin receptor phosphorylation, and cell growth. In the presence of hIGF-II, large complexes of m660 were formed that bound to FcγRII-expressing BJAB cells much more efficiently than the monospecific antibody–hIGF-II complexes and were presumably phagocytosed by phorbol 12-myristate 13-acetate–stimulated macrophage-like U937 cells. A mixture of m610.27 and m630.3 exhibited similar properties. To our knowledge, these mAbs are the first reported to target nonoverlapping epitopes on a cancer-related ligand and could represent a novel class of candidate therapeutics against cancers. This approach could also be used to irreversibly eliminate other disease-related soluble ligands.

Corresponding Author: Dimiter S. Dimitrov, National Cancer Institute (NCI), NIH, Miller Drive, Building 469, Room 150B, Frederick, MD 21702. Phone: 301-846-1352; Fax: 301-846-5598; dimiter.dimitrov@nih.gov.

Authors' Contributions

Conception and design: W. Chen, Y. Feng, D.S. Dimitrov

Development of methodology: W. Chen, Y. Feng, Q. Zhao, Z. Zhu, D.S. Dimitrov

Acquisition of data (provided animals, acquired and managed patients, provided facilities, etc.): W. Chen, Y. Feng, Q. Zhao, D.S. Dimitrov

Analysis and interpretation of data (e.g., statistical analysis, biostatistics, computational analysis): W. Chen, Y. Feng, Q. Zhao, D.S. Dimitrov

Writing, review, and/or revision of the manuscript: W. Chen, Q. Zhao, D.S. Dimitrov

Administrative, technical, or material support (i.e., reporting or organizing data, constructing databases): Y. Feng, Q. Zhao, D.S. Dimitrov

Study supervision: Q. Zhao, D.S. Dimitrov

Note: Supplementary data for this article are available at Molecular Cancer Therapeutics Online (http://mct.aacrjournals.org/).

Disclosure of Potential Conflicts of Interest

No potential conflicts of interest were disclosed.

Introduction

Insulin-like growth factors (IGF), IGF-I and IGF-II, are circulating small soluble ligands (1, 2). They bind to IGF receptor type I (IGF-IR) and activate multiple intracellular signaling pathways resulting in cell proliferation, survival, differentiation, and transformation. IGF-II also binds to insulin receptor (IR), primarily A isoform (IR-A), with high affinity, as well as to hybrid receptors containing IGF-IR and IR chains. Elevated expression of these receptors and/or ligands has been detected in some cancer tissues such as human breast carcinomas and linked to their pathogenesis. Therefore, the IGF-mediated pathways are attractive targets for cancer therapy. Small-molecule tyrosine kinase inhibitors and monoclonal antibodies (mAb) against IGF-IR have shown benefits in human clinical trials (1). However, resistance to the IGF-IR–directed agents has developed (3). A possible mechanism is the involvement of IR when the IGF-IR–mediated pathways are blocked. Thus, targeting both IR and IGF-IR may be necessary to completely inhibit the signal transduction mediated by IGF-II. Although IR is also functionally important for glucose homeostasis, targeting IGF-II may be an ideal strategy, which could leave the insulin–IR interactions unaffected. Recently, several mAbs specific to IGF-II or cross-reactive against IGF-I and IGF-II have been identified that potently inhibit the growth and migration of human cancer cells *in vitro* and *in vivo* (4–8).

Unlike the antibodies against receptors, many of which inhibit tumor growth by modulating ligand–receptor interactions and by receptor downregulation, ligand-specific antibodies could act as carrier proteins and help ligands evade some clearance mechanisms such as renal filtration and proteolytic digestion because of the long half-lives and high stability of antibodies (9, 10). The dissociation of immune complexes would allow for slow release of ligands that continue to function. This possibility has been evidenced by previous studies on cytokines showing that murine mAbs prolonged the serum half-life and bioactivity of human interleukins in mice, although they completely neutralized the interleukins *in vitro* (10–12). Therefore, strategies to eliminate ligands efficiently and irreversibly are desirable to improve the inhibitory activities of antibodies.

An antigen with 2 or more nonoverlapping antibody-binding sites is likely to cross-link antibodies, resulting in large immune complexes that can be cleared as a result of activation of conventional immune clearance mechanisms such as complement deposition and Fc gamma receptor (FcγR)-mediated internalization and degradation (13). In this study, we describe the generation and characterization of 2 human mAbs, m610.27 and m630.3, targeting nonoverlapping epitopes on IGF-II, and a bispecific antibody, m660, based on them. m660 not only inhibited IGF-II–mediated receptor phosphorylation and cancer cell growth but also formed large soluble immune complexes with IGF-II, which were presumably phagocytosed by phorbol 12-myristate 13-acetate (PMA)-stimulated macrophage-like U937 cells, suggesting the same possibility *in vivo*.

Materials and Methods

Cells, plasmids, soluble ligands, antibodies, and phagocytosis inhibitors

The BJAB cells and U937 cells (clone P) were a gift from Anu Puri (National Cancer Institute, Frederick, MD, USA). The MCF-7 cells were obtained from the DCTD Tumor Repository, Frederick National Laboratory for Cancer Research, National Cancer Institute. All the cell lines were previously characterized by others, as reported (14–16); no authentication was done by the authors. Plasmids pComb3X and pDR12 were kindly provided by Dennis Burton (Scripps Research Institute, La Jolla, CA, USA). The 293 free style cells, human insulin, fluorescein isothiocyanate (FITC)-conjugatedmouseanti-humanCD64 (FcγRI), CD32 (FcγRII), and CD16 (FcγRIII) antibodies, and streptavidin–PE conjugate were purchased from Invitrogen. Mature human IGF-I (hIGF-I) and IGF-II (hIGF-II), mouse IGF-II (mIGF-II), and IGF-binding proteins (IGFBP) were purchased from R&D Systems. A precursor form of hIGF-II (long hIGF-II) was produced in our laboratory. Horseradish peroxidase (HRP)-conjugated mouse anti-FLAG tag antibody, HRP-conjugated goat anti-human IgG (Fc-specific) antibody, HRP-conjugated rabbit anti-c-Myc tag antibody, FITC-conjugated goat F(ab')2 anti-human IgG (Fc-specific) antibody, and cytochalasin D were products of Sigma-Aldrich.

Panning and screening of a human engineered antibody domain (eAd) library

To select antibodies noncompeting with a previously reported mAb m610, biotinylated hIGF-II was used to pan a large (size, ~2.5×10^{10}) phage-displayed human eAd library (17) according to the previously described protocol (18). Clones that specifically bound to hIGF-II were identified from the 4th round of panning using soluble expression-based monoclonal ELISA (semELISA) as described previously (19).

Construction, panning, and screening of randomly mutagenized and light chain–shuffled libraries

To affinity mature m630, a phage-displayed library of m630 mutants (size, ~10^9) was constructed. To introduce point mutations, we conducted random DNA mutagenesis with the Gene-Morph PCR Mutagenesis Kit (Stratagene) according to the manufacturer's instructions. m630 gene fragments with mutations were PCR amplified by using m630-encoding plasmid as a template and primers m36F1 (5′-TGGTTTCGCTACCGTGGCCCAGGCGGCCCAGGTGCAGCTGGTG-3′; sense) and HISR (5′-GTCGCCGTGGTGGTGGTGGTGGCCGGCCTGGCCACTTG-3′; antisense). The PCR products were gel-purified, digested with *Sfi*I, and gel-purified again. The purified fragments were then cloned into pComb3X linearized by SfiI. A phage library was prepared by electroporation of *Escherichia coli* (*E. coli*) strain TG1 electroporation-competent cells (Stratagene) with desalted and concentrated ligation, as described previously (17). The phage library was panned against hIGF-II coated on 96-well plates as described (5). Clones that bound to hIGF-II were identified from the third round of panning using semELISA.

To affinity mature m610, a light chain–shuffled antigen-binding fragment (Fab) library (size, ~10^8) was constructed on the basis of the heavy chain of m610 according to the reported

protocols (20). The light chain repertoire was harvested from a naive human Fab library (size, ~5×10^9) constructed from peripheral blood B cells of 10 healthy donors (21). The new library was panned against hIGF-II coated on 96-well plates and screened for higher affinity binders using monoclonal phage ELISA (mpE-LISA) as described previously (21).

Cloning of fusion proteins

The following primers were used: m36F, 5′-TGGTTTCGCTACCGTGGCCCAGCCGGCCCAGGTGCAGCTGGTG-3′ (sense); m36R1, 5′-GTGAGTTTTGTCGGGCCCTGAGGAGACGGTGAC-3′ (antisense); bnIgG20H1, 5′-GTGTTCTAGAGCCGCCACCATGGAATGGAGCTGGGTCTTTCTCTTC-3′ (sense); bnIgG20H3, 5′-GGAGTGGACACCTGTAGTTACTGACAGGAAGAAGAGAAAGAC-3′ (antisense); m610.27H2, 5′-ACTACAGGTGTCCACTCCCAAGTGCAGCTGGTGCAG-3′ (sense); m610.27-H4, 5′-CCTTGGAGCTCGATCCGCCACCGCCAGAGCCACCTCCGCCTGAACCGCCTCCACCTCGTTTGATCTCCACC-3′ (antisense); m36.4L2, 5′-CTTACAGATGCCAGATGTCAGGTGCAGCTGGTGCAG-3′ (sense); m36.4L4, 5′-AGAGCCACCTCCGCCTGAACCGCCTCCACCTGAGGAGACGGTGACCAG-3′ (antisense); bnIgG20L1, 5′-GTGTAAGCTTACCATGGGTGTGCCCACTCAGGTCCTGGGGTTGCTG-3′ (sense); bnIgG20L3, 5′-ACATCTGGCATCTGTAAGCCACAGCAGCAGCAACCCCAGGAC-3′ (antisense); CLF, 5′-TCAGGCGGAGGTGGCTCTGGCGGTGGCGGATCACGAACTGTGGCTGCACCA-3′ (sense); and bnIgG20L4, 5′-GTGTGAATTCATTAACACTCTCCCCTGTTGAA-3′ (antisense).

IgG1 m610.27 was constructed by cloning Fab m610.27 into pDR12, which allows simultaneous expression of the heavy and light chains using protocols and reagents similar to those we used previously (5). Briefly, the heavy chain variable region was first cloned into pDR12 via *Xba*I and *Sac*I sites. The light chain sequence was then cloned into pDR12 via *Hin*dIII and *Eco*RI sites. To clone m630.3Fc, m630.3 gene fragment was PCR-amplified with primers m36F and m36R1, digested with *Sfi*I and *Apa*I, and cloned into pSecTagB-Fc. To generate the bispecific antibody m660, the heavy chain leader peptide gene fragment (Hleader) and the single-chain variable fragment (scFv) of m610.27 were PCR-amplified with primer pairs bnIgG20H1/bnIgG20H3 and m610.27H2/m610.27H4, respectively. Hleader was joined to scFv m610.27 by overlapping PCR conducted in a volume of 50 μL by using both templates (in the same molarities) for 7 cycles in the absence of primers and 15 additional cycles in the presence of primers (500 pmol/L of bnIgG20H1 and m610.27H4). The product was digested with *Xba*I and *Sac*I, and cloned into pDR12. To fuse m630.3 to the N terminus of the human IgG1 light chain constant region, the light chain leader peptide (Lleader), m630.3, and the human IgG1 kappa light chain constant region (CK) were amplified by PCR with primer pairs bnIgG20L1/bnIgG20L3, m36.4L2/m36.4L4, and CLF/bnIgG20L4, respectively. Lleader was linked to m630.3 and CK by overlapping PCR with primers bnIgG20L1 and bnIgG20L4 as described earlier. The Lleader–m630.3–

CK fragment was then digested with *Eco*RI and *Hin*dIII, and cloned into the pDR12 construct containing scFv m610.27.

Protein expression and purification

Fabs and eAds were expressed and purified from *E. coli* HB2151 periplasm, and all fusion proteins were produced in 293 free style cells, as described previously (22).

Size exclusion chromatography

Size exclusion chromatography was done as described previously (23) except a Superdex200 10/300 GL column (GE Healthcare) was used in this study.

ELISA

ELISA was done as described previously (22). Bound Fabs and eAds were detected by HRP-conjugated mouse anti-FLAG tag antibody. The antibody–Fc fusion proteins binding to IGF-II directly coated on 96-well plates were detected by HRP-conjugated goat anti-human IgG (Fc-specific) antibody. In the competition ELISA with IGF-II captured by IgG1s, bound m630.3Fc was detected by HRP-conjugated rabbit anti-c-Myc tag antibody. In the competition ELISA with IGF-II captured by IGFBPs, bound antibodies were detected by HRP-conjugated goat anti-human IgG (Fc-specific) antibody. The half-maximal binding (EC_{50}) was calculated by fitting the data to the Langmuir adsorption isotherm.

Flow cytometry (FACS)

To measure the interactions of IGF-II with MCF-7, BJAB and U937 cells, biotinylated IGF-II was mixed with or without antibodies and added to approximately 10^5 cells in 200 μL PBS containing 0.1% BSA (PBSA). After 1-hour incubation on ice, the cells were washed twice and resuspended in 200 μL PBSA, and 1 mL streptavidin–PE conjugate was added. Following 30-minute incubation on ice, the cells were washed twice and then subjected to fluorescence-activated cell sorting (FACS). For detection of the expression of FcγRII and FcγRI, 10^5 BJAB and PMA-stimulated U937 cells in 200 μL PBSA were mixed at different ratios (v/v) with FITC-conjugated mouse anti-human CD32 (FcγRII) and CD64 (FcγRI) antibodies, respectively, and incubated for 30 minute on ice. The cells were washed twice with 200 μL PBSA and then used for FACS analysis. Antibody binding to BJAB and U937 cells in the absence or presence of IGF-II was detected by FITC-conjugated goat F(ab')2 anti-human IgG (Fc-specific) antibody at a 1:200 dilution (v/v).

Phosphorylation assay

Inhibition of IGF-II–mediated receptor phosphorylation by the antibodies was measured as described previously (5).

Cell growth assay

Cell growth assay was done as described previously (5) except that live cells were determined by using the CellTiter-Glo® Luminescent Cell Viability Assay System (Promega) according to the manufacturer's instructions.

Results

Selection and affinity maturation of IGF-II–specific mAbs

We identified previously a human mAb to IGF-II, m610, which potently inhibited IGF-IR and IR signaling pathways and cancer cell growth *in vitro* (5) and in a mouse model with implanted human bone (6). To further increase its affinity, an Fab library with shuffled light chains was generated and panned against hIGF-II. One of the mutants selected, m610.27, had a light chain derived from the same germline (IGKV1–39*01) but with 8 mutations compared with the original; its heavy chain remained the same as m610 that was closest to the family IGHV1–46*01 (Supplementary Fig. S1A). m610.27 in Fab format bound to hIGF-II with an EC_{50} of 5 nmol/L, 4-fold lower than that (20 nmol/L) of m610 (data not shown). We also identified a novel eAd, m630, by panning and screening one of our large phage-displayed eAd libraries against hIGF-II. m630 did not compete with m610 in binding to hIGF-II and mIGF-II in ELISA-based assays (data not shown). m630 was affinity matured by panning and screening of a phage-displayed library generated by random mutagenesis with error-prone PCR. Four m630 mutants, designated m630.1, m630.3, m630.4, and m630.9, were selected (Supplementary Fig. S1B). The highest affinity binder, m630.3, bound to hIGF-II with an EC_{50} (2 nmol/L) 25-fold lower than that (50 nmol/L) of m630 (data not shown).

Generation and characterization of monospecific and bispecific IgG1-like mAbs

Fab m610.27 was converted to an IgG1 (Supplementary Fig. S2A). A fusion protein, m630.3Fc, was made by attaching m630.3 to the N terminus of a human IgG1 Fc via a hinge (Supplementary Fig. S2B). An IgG1-like bispecific antibody, m660, was generated by fusing scFv m610.27 and m630.3 to the N termini of the heavy and light chain constant regions of a human IgG1, respectively, via a linker composed of 3 repeats of the G_4S motif (Supplementary Fig. S2C). IgG1 m610.27, m630.3Fc, and m660 were well expressed and purified from 293 free style cell culture supernatants with yields of 5.5, 12, and 2.0 mg/L, respectively. They migrated on a SDS-PAGE under reducing and nonreducing conditions with apparent molecular weights (aMWs) comparable with their calculated molecular weights (cMWs) or slightly higher because of glycosylation (Supplementary Fig. S2D).

Binding activity and specificity of the antibodies were analyzed by ELISA. m630.3Fc bound to hIGF-II directly coated on 96-well plates with an EC_{50} (0.6 nmol/L) about 6-fold lower than that (3.5 nmol/L) of IgG1 m610.27 (Fig. 1A). It was cross-reactive against hIGF-I although very weakly while no significant binding of IgG1 m610.27 to hIGF-I was observed at a concentration up to several mmol/L. Neither m630.3Fc nor IgG1 m610.27 interacted measurably with human insulin. Both antibodies bound strongly to mIGF-II with an EC_{50} of 0.7 nmol/L for m630.3Fc and 8 nmol/L for IgG1 m610.27 (Fig. 1B). As expected for noncompeting antibodies, m630.3Fc bound to the hIGF-II (Fig. 1C) and mIGF-II (Fig. 1D) captured by IgG1 m610.27. In contrast, it did not bind to the IGF-II captured by IgG1 m708.5 (24), which is a human mAb cross-reactive to hIGF-I and hIGF-II, suggesting a competitive binding of m630.3Fc with IgG1 m708.5. m660 bound to hIGF-II with an EC_{50} comparable to that of m630.3Fc and 3-fold lower than that of IgG1 m610.27 (Fig. 1E). To find out whether the lack of additional avidity effects of m660 could be because of the

possible inaccessibility of one of the antibody epitopes, we used long hIGF-II, which provides larger surface areas for coating. m660 exhibited stronger binding to long hIGF-II than both monospecific antibodies (Fig. 1F). We further tested the possible interaction of the antibodies with IGF-II/IGFBP complexes, which represent >90% of the forms of IGF-II in humans. m630.3Fc showed no detectable binding to the hIGF-II captured by IGFBP2 (Fig. 1G) or IGFBP3 (Fig. 1H), which were coated on 96-well plates. In contrast, IgG1 m610.27 strongly bound to the captured hIGF-II with EC_{50}s comparable to that of the antibody with hIGF-II directly coated on 96-well plates (Fig. 1A), suggesting that the antibody epitope does not overlap with the IGFBP2- and IGFBP3-binding sites. m660 displayed a decreased binding activity against the captured hIGF-II compared with IgG1 m610.27.

Inhibition of hIGF-II binding, receptor phosphorylation, and cancer cell growth

Signaling mediated by IGF-IR and IR is initiated by binding of their ligands. To test whether our antibodies could efficiently block the binding, we incubated MCF-7 cells, which are known to express high levels of IGF-IR, with 1 nmol/L hIGF-II in the absence or presence of the antibodies at different concentrations. At 2 nmol/L antibody concentration, m630.3Fc did not show any significant inhibition in a flow cytometry–based assay (Fig. 2). IgG1 m610.27, m660, and IgG1 m610.27 mixed with the same molar concentration of m630.3Fc completely inhibited the binding. m660 at 1 nmol/L still gave 100% inhibition whereas reduced inhibitory activity was observed with IgG1 m610.27 alone or in combination with m630.3Fc at the same concentration.

Upon ligand binding, IGF-IR undergoes phosphorylation on tyrosine residues of the 2 β-subunits. To find out whether the antibodies could inhibit the transmembrane signaling mediated by IGF-IR, we measured the receptor phosphorylation in MCF-7 cells. Although the serum concentration of free IGF-II in healthy individuals is approximately 2.3 nmol/L according to a previous study (25) and the half-maximal effective dose (EC_{50}) of IGF-II to mediate receptor phosphorylation could be even lower, we used 5 nmol/L or higher IGF-II concentrations in this and our previous studies (5, 24) because the levels of free IGF-II in some patients with cancer could be higher than those in healthy individuals. MCF-7 cells kept in serum-free DMEM displayed nondetectable phosphorylation of IGF-IR (Fig. 3A). After incubation with 5 nmol/L hIGF-II for 30 minutes, the phosphorylation of IGF-IR was readily detected. In the presence of 5 nmol/L m660, however, the phosphorylation was completely inhibited. IgG1 m610.27 and a mixture of IgG1 m610.27 with m630.3Fc at 5 nmol/L also gave strong but incomplete inhibition. m630.3Fc showed no obvious inhibitory activity at the same concentration. When 1 nmol/L antibody concentration was tested, no significant inhibition was seen in all cases. In addition to IGF-IR, IGF-II also binds to and activates IR. As shown in Fig. 3A, m660, IgG1 m610.7, or IgG1 m610.27 plus m630.3Fc at 5 nmol/L completely blocked the effects of 5 nmol/L hIGF-II on IR phosphorylation. Marked inhibition was also observed when the antibody concentration was decreased to 1 nmol/L. m630.3Fc seems to slightly inhibit IR phosphorylation but its effect was not concentration-dependent.

To find out whether the antibodies could inhibit cell proliferation, we used MCF-7 cells in a cell growth assay. m630.3Fc at a concentration of 200 nmol/L did not measurably affect the

growth of the cells incubated with 10 nmol/L hIGF-II (Fig. 3B). By comparison, m660 ($P < 0.001$), IgG1 m610.27 alone ($P = 0.017$) or mixed with m630.3Fc at the same concentration ($P = 0.002$) exhibited potent inhibitory activity with IC_{50}s of 1.6 to 8 nmol/L. However, none of the 3 groups was significantly better than the others ($P > 0.05$).

Formation of large soluble m660–IGF-II complexes and enhanced interaction with FcγRII-expressing cells

Multivalent antibody–antigen interactions can induce formation of large immune complexes that either precipitate or remain soluble, depending on the degrees to which antigens are cross-linked by antibodies. To find out whether large m660–IGF-II complexes could be formed, m660 was mixed with hIGF-II at different molar ratios and analyzed by size exclusion chromatography. m660 alone was monomeric with aMW of approximately 180 kDa (Fig. 4). With hIGF-II at the same molar concentration, about one-half of m660 eluted as a dimer with aMW of approximately 380 kDa; a small percentage of the antibody was trimerized and eluted at a position corresponding to an aMW of 580 kDa. When the m660:hIGF-II ratio was changed to 1:2, the antibody monomer quantity decreased significantly and larger amounts of trimer were observed. With a further increase of the amount of hIGF-II (ratio 1:4 or 1:8), almost all the antibody was in a trimeric state. To test whether the presence of IGFBP would affect the formation of the complexes, we used a mixture of m660, hIGF-II, and IGFBP3 at a 1:4:2 ratio. IGFBP3 was first mixed with hIGF-II. Following 30-minute incubation on ice, m660 was then added. The result showed that about 30% of the antibody was in a dimeric state while the rest eluted as a monomer (Fig. 4). The elution peak corresponding to the antibody dimer showed a shift compared to those in the absence of IGFBP3, suggesting the engagement of IGFBP3 in the complexes. In all cases, no precipitation was observed. Similar complexation was observed when m660 was replaced with IgG1 m610.27 plus m630.3Fc at an equal molar concentration (data not shown). However, when hIGF-II was mixed with either IgG1 m610.27 or m630.3Fc, they eluted at positions similar to those for the antibodies alone, suggesting no cross-linking between the monospecific antibodies and hIGF-II (data not shown).

Large antibody–antigen complexes are able to trigger immune clearance mechanisms with efficient recognition of multiple antibody Fc domains by effector cells expressing FcγRs because of avidity effects. To determine the effects of m660 oligomerization through cross-linking of IGF-II, we used as a model BJAB cells, a human B cell line. According to a previous study (26), B cells express only FcγRII, which weakly (equilibrium dissociation constant of approximately 1 μmol/L) binds to naturally occurring antibodies with monovalent Fc. Therefore, the differences in binding between m660–IGF-II and monospecific antibody–IGF-II complexes could be better observed by using this cell line. Our results from flow cytometry analysis confirmed the expression of FcγRII using the FITC-conjugated mouse anti-human FcγRII and FcγRIII antibodies (Fig. 5A). We also found that BJAB cells did not significantly interact with hIGF-II at a concentration up to 1 μmol/L (Fig. 5B). Monospecific antibody IgG1 m610.27 or m630.3Fc showed weak interactions with BJAB cells and their binding was not or only slightly altered when hIGF-II was added at a 1:2 molar ratio (antibody:hIGF-II; Fig. 5C). As expected, the presence of hIGF-II at a 1:4 ratio dramatically enhanced the interactions of m660 or IgG1 m610.27 plus

m630.3Fc at an equal molar concentration with the cells (Fig. 5C). hIGF-II did not significantly affect the control antibodies IgG1 m102.4, a human mAb specific for henipaviruses (21), plus m36h1Fc, an antibody–Fc fusion protein against HIV-1 (22), in binding to BJAB cells.

Presumably enhanced phagocytosis of m660–IGF-II complexes by macrophage-like U937 cells

Macrophage-mediated phagocytosis is one of the mechanisms for clearance of pathogens, cellular debris, and large immune complexes *in vivo*. To see whether m660–IGF-II complexes could activate this mechanism, we used PMA-stimulated macrophage-like U937 cells, which express considerable levels of FcγRI (Fig. 6A). The cells strongly interacted with hIGF-II alone at various concentrations suggesting the expression of IGF-IR and/or IR on the cell surface (Fig. 6B). To detect the interactions of the antibodies with or without hIGF-II, we used an FITC-conjugated goat F(ab')2 anti-human IgG (Fc-specific) antibody. In a flow cytometry–based assay, in which the antibodies were incubated with the cells on ice for 1 hour, the presence of 20 nmol/L hIGF-II slightly decreased or did not alter the binding of 10 nmol/L IgG1 m610.27 and m630.3Fc to the cells (Fig. 6C). In contrast to the enhanced interactions with BJAB cells, however, increased binding of m660 at 10 nmol/L to U937 cells was not observed in the presence of 40 nmol/L hIGF-II. In the other assay, we incubated the antibodies with the cells at 37°C for 2 hours where phagocytosis is supposed to be more efficient than at 4°C. Although hIGF-II did not affect the interactions of the monospecific antibodies, m660 binding strength was decreased by approximately 80%, indicating internalization of the receptor/IGF-II/antibody complexes. To further assess the possibility of phagocytosis, we applied 50 μmol/L cytochalasin D, a phagocytosis inhibitor, to both thermal conditions. As expected, binding of m660 was increased at 4°C and partially restored at 37°C whereas cytochalasin D impaired the monospecific antibody binding.

Discussion

Soluble ligands are important targets for therapy of many diseases. In this study, we used IGF-II as a model to test our hypothesis that mAbs targeting nonoverlapping epitopes on a single ligand molecule are capable of driving the formation of large soluble immune complexes, which, because of avidity effects of multivalent Fc, could activate the immune clearance mechanisms *in vivo* leading to efficient and irreversible removal of ligands from the circulation.

Our results from the size exclusion chromatography showed that at an antibody-hIGF-II ratio of 1:4 or higher, almost all m660 was in trimeric states (Fig. 4). The level of antibody–antigen complexation could be affected by a number of other factors including the orientations of epitopes and paratopes, and the relative affinity of binding moieties. In humans, the complexation could be further affected by the existence of a large amount of IGF-II in complex with IGFBPs and acid labile subunit (ALS; ref. 27). Our results showed that the m610.27 arm of m660 was able to interact with IGF-II/IGFBP complexes (Fig. 1G and 1H) and an addition of IGFBP3 resulted in a reduced level of antibody cross-linking (Fig. 4). However, whether m610.27 would bind to the IGF-II/IGFBP/ALS binary

complexes remains unknown. We did not test the effects of ALS because of the difficulty of obtaining soluble functional ALS. The m630.3 arm of m660 bound to free IGF-II only, which will ensure the formation of large immune complexes albeit to a lesser extent because of the low concentration of free IGF-II *in vivo*. However, the removal of free IGF-II would lead to a shift in the equilibrium between free and complexed IGF-II, which finally may result in complete irreversible depletion of total IGF-II. A note of concern is the possibility for side effects because of the complexation. It is known that immune complex deposition is a prominent feature of several autoimmune diseases such as the systemic lupus erythematosus (28). However, the serum concentration of IGF-II is relatively low leading to a relatively low rate of their formation so such possibility seems unlikely.

The binding avidity of large m660–hIGF-II complexes was shown by using BJAB cells, a human B lymphoma cell line (Fig. 5). Although mammalian B cells lack phagocytic capabilities, previous studies showed that they could preferentially uptake antigen–antibody complexes through FcγRII-mediated endocytosis (29). Moreover, there is supporting evidence that B cells evolve from an ancestral phagocytic cell type (30). These findings indicate a previously unknown function of B cells in the innate immunity of mammals. Other cell types expressing FcγRII or FcγRIII may also have similar activities especially when large immune complexes with multivalent Fc are presented. Figure 6 showed that after incubation of m660-hIGF-II complexes with PMA-stimulated macrophage-like U937 cells at 37°C for 2 hours, the antibody binding strength was decreased by approximately 80% whereas no significant decrease in binding was observed in the control groups (monospecific antibodies mixed with hIGF-II). Moreover, phagocytosis inhibitor cytochalasin D enhanced binding of m660–hIGF-II but not the monospecific antibody–hIGF-II complexes to the cells. These results suggest that the Fc receptors on the cells incubated with m660–hIGF-II complexes could be down-regulated presumably by co-internalization with the complexes.

One of the advantages of antibodies capable of irreversibly removing soluble ligands (iAbs) compared with reversible blocking antibodies (rAbs), could be that the former may function efficiently even with relatively low nmol/L affinity. Although the interactions between a receptor and iAbs competing for a ligand *in vivo* are complex, one could assume that following iAb administration, the total concentration of soluble ligand (in this case, IGF-II) should be gradually decreased to levels much lower than those achievable with rAbs. In contrast, rAbs tend to increase ligand concentrations because of the long half-lives of the antibodies, which serve as a reservoir. As a result, high pmol/L affinity is generally required for rAbs to efficiently block receptor–ligand interactions whereas low nmol/L affinity may be sufficient for iAbs efficacy. Our results showed that *in vitro*, the IGF-IR and IR phosphorylation mediated by hIGF-II at 5 nmol/L, a concentration higher than its average physiological concentration in healthy individuals (2.3 nmol/L), was 100% inhibited by the bispecific iAb m660 at 5 nmol/L final concentration (Fig. 3A). Typically, therapeutic antibody concentrations in the circulation are much higher (on the order of 1,000 nmol/L); therefore, we could expect that our antibodies would be capable of preventing signal transduction *in vivo*.

Further studies in animal models and humans are needed to find out whether m660 or a mixture of m610.27 with m630.3 could have potential as candidate human IGF-related

cancer therapeutics. The antibodies can be used alone or in combinations with IGF-IR-directed agents and other antitumor therapeutics.

Supplementary Material

Refer to Web version on PubMed Central for supplementary material.

Acknowledgments

The authors thank Anu Puri for providing cells and John Owens for technical assistance.

Grant Support

This work was supported by the Intramural Research Program of the NIH, National Cancer Institute, Frederick National Laboratory for Cancer Research (D.S. Dimitrov).

The costs of publication of this article were defrayed in part by the payment of page charges. This article must therefore be hereby marked *advertisement* in accordance with 18 U.S.C. Section 1734 solely to indicate this fact.

References

1. Ryan PD, Goss PE. The emerging role of the insulin-like growth factor pathway as a therapeutic target in cancer. Oncologist 2008;13:16–24.
2. Samani AA, Yakar S, LeRoith D, Brodt P. The role of the IGF system in cancer growth and metastasis: overview and recent insights. Endocr Rev 2007;28:20–47. [PubMed: 16931767]
3. Hendrickson AW, Haluska P. Resistance pathways relevant to insulin-like growth factor-1 receptor-targeted therapy. Curr Opin Investig Drugs 2009;10:1032–40.
4. Goya M, Miyamoto S, Nagai K, Ohki Y, Nakamura K, Shitara K, et al. Growth inhibition of human prostate cancer cells in human adult bone implanted into nonobese diabetic/severe combined immunodeficient mice by a ligand-specific antibody to human insulin-like growth factors. Cancer Res 2004;64:6252–8. [PubMed: 15342412]
5. Feng Y, Zhu Z, Xiao X, Choudhry V, Barrett JC, Dimitrov DS. Novel human monoclonal antibodies to insulin-like growth factor (IGF)-II that potently inhibit the IGF receptor type I signal transduction function. Mol Cancer Ther 2006;5:114–20. [PubMed: 16432169]
6. Kimura T, Kuwata T, Ashimine S, Yamazaki M, Yamauchi C, Nagai K, et al. Targeting of bone-derived insulin-like growth factor-II by a human neutralizing antibody suppresses the growth of prostate cancer cells in a human bone environment. Clin Cancer Res 2010;16:121–9. [PubMed: 20028742]
7. Dransfield DT, Cohen EH, Chang Q, Sparrow LG, Bentley JD, Dolezal O, et al. A human monoclonal antibody against insulin-like growth factor-II blocks the growth of human hepatocellular carcinoma cell lines *in vitro* and *in vivo*. Mol Cancer Ther 2010;9:1809–19. [PubMed: 20515953]
8. Gao J, Chesebrough JW, Cartlidge SA, Ricketts SA, Incognito L, Veldman-Jones M, et al. Dual IGF-I/II-neutralizing antibody MEDI-573 potently inhibits IGF signaling and tumor growth. Cancer Res 2011;71:1029–40. [PubMed: 21245093]
9. Rehlaender BN, Cho MJ. Anti-drug antibodies as drug carriers. I. For small molecules. Pharm Res 2001;18:745–52. [PubMed: 11474777]
10. Mihara M, Koishihara Y, Fukui H, Yasukawa K, Ohsugi Y. Murine anti-human IL-6 monoclonal antibody prolongs the half-life in circulating blood and thus prolongs the bioactivity of human IL-6 in mice. Immunology 1991;74:55–9. [PubMed: 1718855]
11. Finkelman FD, Madden KB, Morris SC, Holmes JM, Boiani N, Katona IM, et al. Anti-cytokine antibodies as carrier proteins. Prolongation of *in vivo* effects of exogenous cytokines by injection of cytokine-anti-cytokine antibody complexes. J Immunol 1993;151: 1235–44. [PubMed: 8393043]

12. May LT, Neta R, Moldawer LL, Kenney JS, Patel K, Sehgal PB. Antibodies chaperone circulating IL-6. Paradoxical effects of anti-IL-6 “neutralizing” antibodies *in vivo*. J Immunol 1993;151:3225–36. [PubMed: 8376777]
13. Gessner JE, Heiken H, Tamm A, Schmidt RE. The IgG Fc receptor family. Ann Hematol 1998;76:231–48. [PubMed: 9692811]
14. Klein G, Lindahl T, Jondal M, Leibold W, Menezes J, Nilsson K, et al. Continuous lymphoid cell lines with characteristics of B cells (bone-marrow-derived), lacking the Epstein-Barr virus genome and derived from three human lymphomas. Proc Natl Acad Sci U S A 1974;71: 3283–6. [PubMed: 4369887]
15. Smith SD, Shatsky M, Cohen PS, Warnke R, Link MP, Glader BE. Monoclonal antibody and enzymatic profiles of human malignant T-lymphoid cells and derived cell lines. Cancer Res 1984;44: 5657–60. [PubMed: 6437672]
16. Soule HD, Vazguez J, Long A, Albert S, Brennan M. A human cell line from a pleural effusion derived from a breast carcinoma. J Natl Cancer Inst 1973;51:1409–16. [PubMed: 4357757]
17. Chen W, Zhu Z, Feng Y, Xiao X, Dimitrov DS. Construction of a large phage-displayed human antibody domain library with a scaffold based on a newly identified highly soluble, stable heavy chain variable domain. J Mol Biol 2008;382:779–89. [PubMed: 18687338]
18. Zhang MY, Shu Y, Phogat S, Xiao X, Cham F, Bouma P, et al. Broadly cross-reactive HIV neutralizing human monoclonal antibody Fab selected by sequential antigen panning of a phage display library. J Immunol Methods 2003;283:17–25. [PubMed: 14659896]
19. Chen W, Zhu Z, Feng Y, Dimitrov DS. A large human domain antibody library combining heavy and light chain CDR3 diversity. Mol Immunol 2010;47:912–21. [PubMed: 19883941]
20. Zhu Z, Dimitrov DS. Construction of a large naive human phage-displayed Fab library through one-step cloning. Methods Mol Biol 2009;525:129–42, xv. [PubMed: 19252833]
21. Zhu Z, Dimitrov AS, Bossart KN, Crameri G, Bishop KA, Choudhry V, et al. Potent neutralization of Hendra and Nipah viruses by human monoclonal antibodies. J Virol 2006;80:891–9. [PubMed: 16378991]
22. Chen W, Zhu Z, Feng Y, Dimitrov DS. Human domain antibodies to conserved sterically restricted regions on gp120 as exceptionally potent cross-reactive HIV-1 neutralizers. Proc Natl Acad Sci U S A 2008;105:17121–6. [PubMed: 18957538]
23. Chen W, Feng Y, Gong R, Zhu Z, Wang Y, Zhao Q, et al. Engineered single human CD4 domains as potent HIV-1 inhibitors and components of vaccine immunogens. J Virol 2011;85:9395–405. [PubMed: 21715496]
24. Zhao Q, Feng Y, Zhu Z, Dimitrov DS. Human monoclonal antibody fragments binding to insulin-like growth factors I and II with picomolar affinity. Mol Cancer Ther 2011;10:1677–85. [PubMed: 21750218]
25. Singer CF, Mogg M, Koestler W, Pacher M, Marton E, Kubista E, et al. Insulin-like growth factor (IGF)-I and IGF-II serum concentrations in patients with benign and malignant breast lesions: free IGF-II is correlated with breast cancer size. Clin Cancer Res 2004;10:4003–9. [PubMed: 15217931]
26. Fridman WH. Fc receptors and immunoglobulin binding factors. FASEB J 1991;5:2684–90. [PubMed: 1916092]
27. Boisclair YR, Rhoads RP, Ueki I, Wang J, Ooi GT. The acid-labile subunit (ALS) of the 150 kDa IGF-binding protein complex: an important but forgotten component of the circulating IGF system. J Endocrinol 2001;170:63–70. [PubMed: 11431138]
28. Childs SG. The pathogenesis of systemic lupus erythematosus. Orthop Nurs 2006;25:140–5; quiz 146–7. [PubMed: 16572034]
29. Berg M, Uellner R, Langhorne J. Fc gamma receptor II dependency of enhanced presentation of major histocompatibility complex class II peptides by a B cell lymphoma. Eur J Immunol 1997;27:1022–8. [PubMed: 9130659]
30. Li J, Barreda DR, Zhang YA, Boshra H, Gelman AE, Lapatra S, et al. B lymphocytes from early vertebrates have potent phagocytic and microbicidal abilities. Nat Immunol 2006;7:1116–24. [PubMed: 16980980]

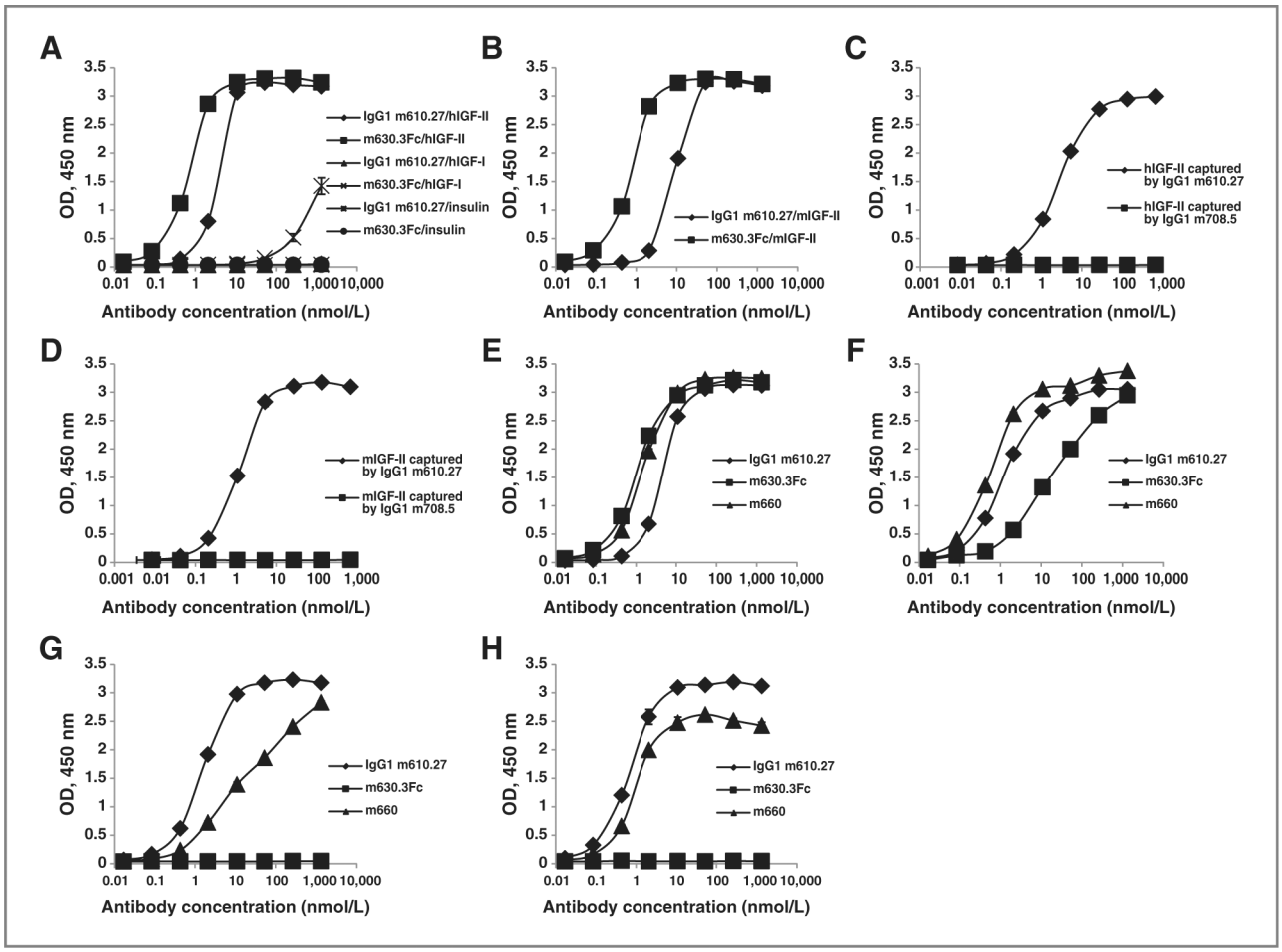

Figure 1.

Binding and competition ELISA. A, binding of IgG1 m610.27 and m630.3Fc to hIGF-II, hIGF-I, and human insulin. B, binding of the antibodies to mIGF-II. C, competition of m630.3Fc with IgG1s m610.27 and m708.5 in binding to hIGF-II. D, competition of m630.3Fc with IgG1s m610.27 and m708.5 in binding to mIGF-II. E, binding of m660 to hIGF-II. F, binding of m660 to long hIGF-II. G, competition of the antibodies with IGFBP2 in binding to hIGF-II. H, competition of the antibodies with IGFBP3 in binding to hIGF-II. All assays were done in duplicate. Error bars were included in all binding curves.

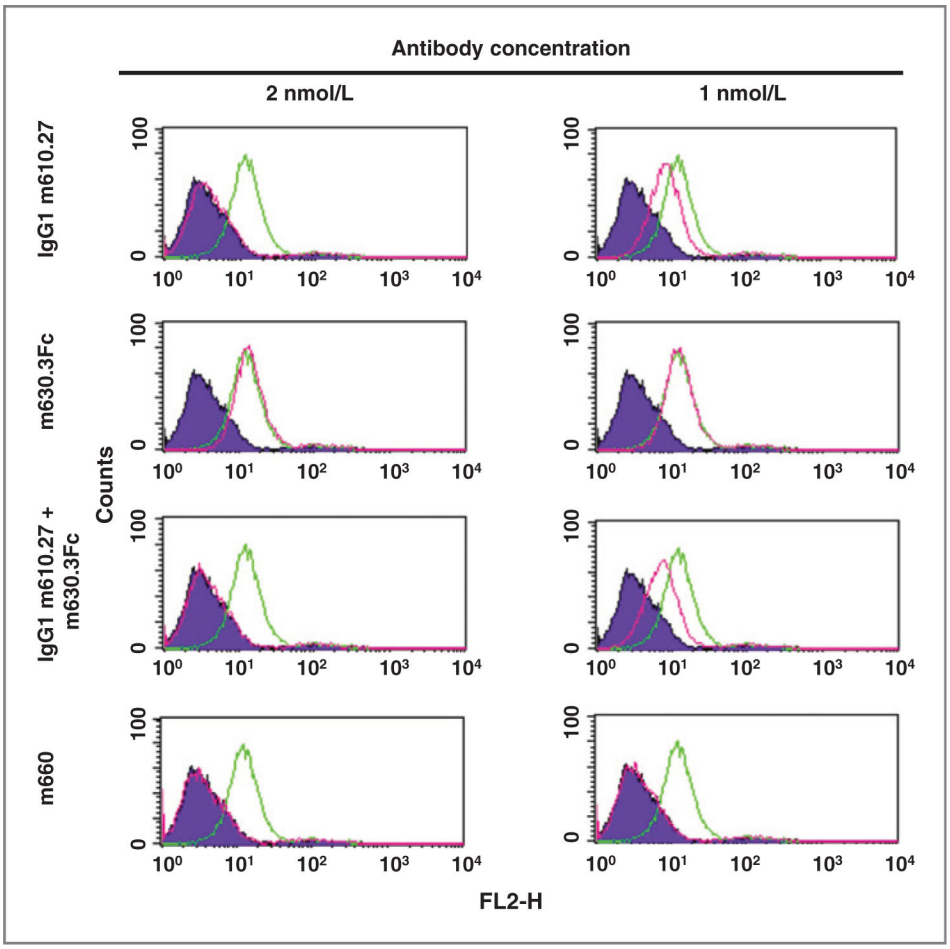

Figure 2.

Inhibition of FACS binding of hIGF-II to MCF-7 cells. Diagrams for reference cells, which were incubated with streptavidin-PE conjugate only, are in purple. Diagrams for cells incubated with hIGF-II only are in green. Those for hIGF-II plus antibodies are in pink.

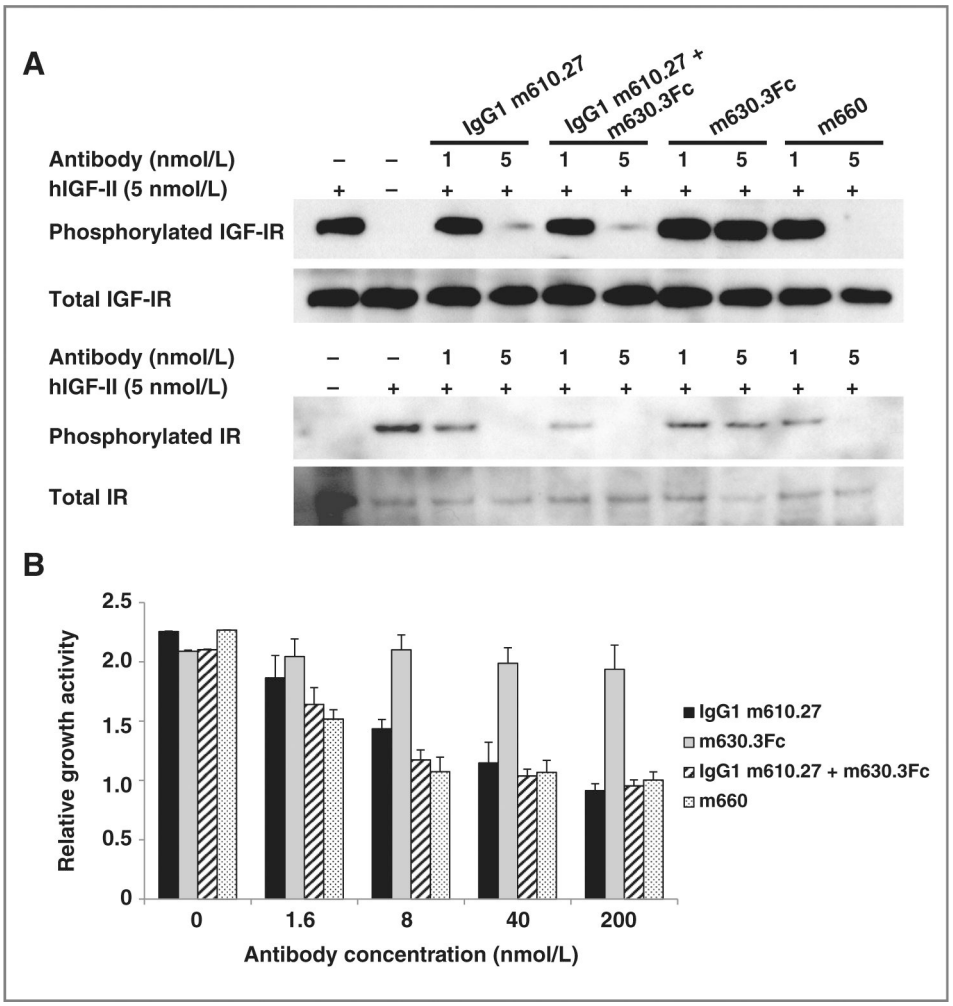

Figure 3.

Inhibition of hIGF-II–mediated IGF-IR and IR phosphorylation (A), and MCF-7 cell growth (B). In the phosphorylation assay, MCF-7 cells were starved in serum-free medium for 5 hours, followed by addition of treatment medium containing 5 nmol/L hIGF-II without or with the antibodies at different concentrations. After 30-minute incubation, cells were chilled and lysed. IGF-IR or IR was immunoprecipitated, and the phosphorylated receptor was detected with a phospho-tyrosine–specific antibody. The membranes were stripped and reprobed by the same polyclonal antibody used for the immunoprecipitation to detect the total amount of the receptors. In the cell growth assay, mean relative light units (RLU) for duplicate wells were determined. Relative growth activity of the cells was calculated by the following formula: average RLU of hIGF-II–containing wells/average RLU of hIGF-II–free wells.

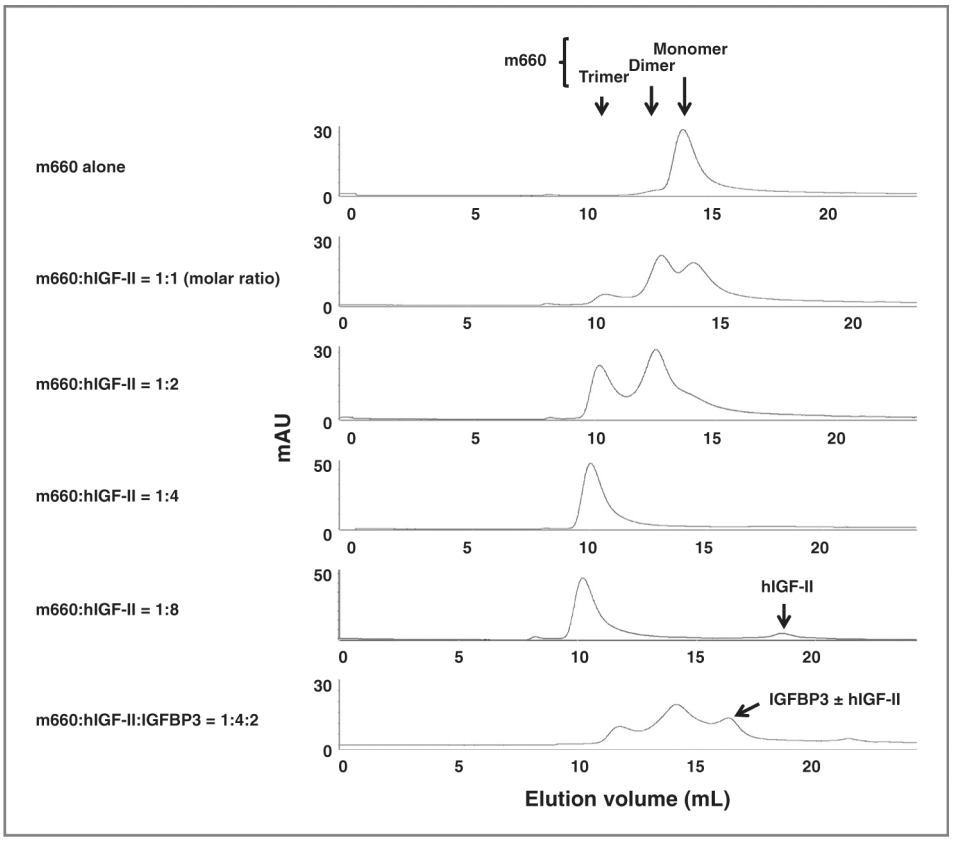

Figure 4.

Size exclusion chromatography analysis of m660–hIGF-II complexes. The bold arrows shown at the top indicate the positions where a monomer, dimer, or trimer of m660 should elute. The bold arrows at the bottom indicate the peaks corresponding to the elution of free hIGF-II and IGFBP3 alone or in complex with hIGF-II, respectively. The ± denotes with or without.

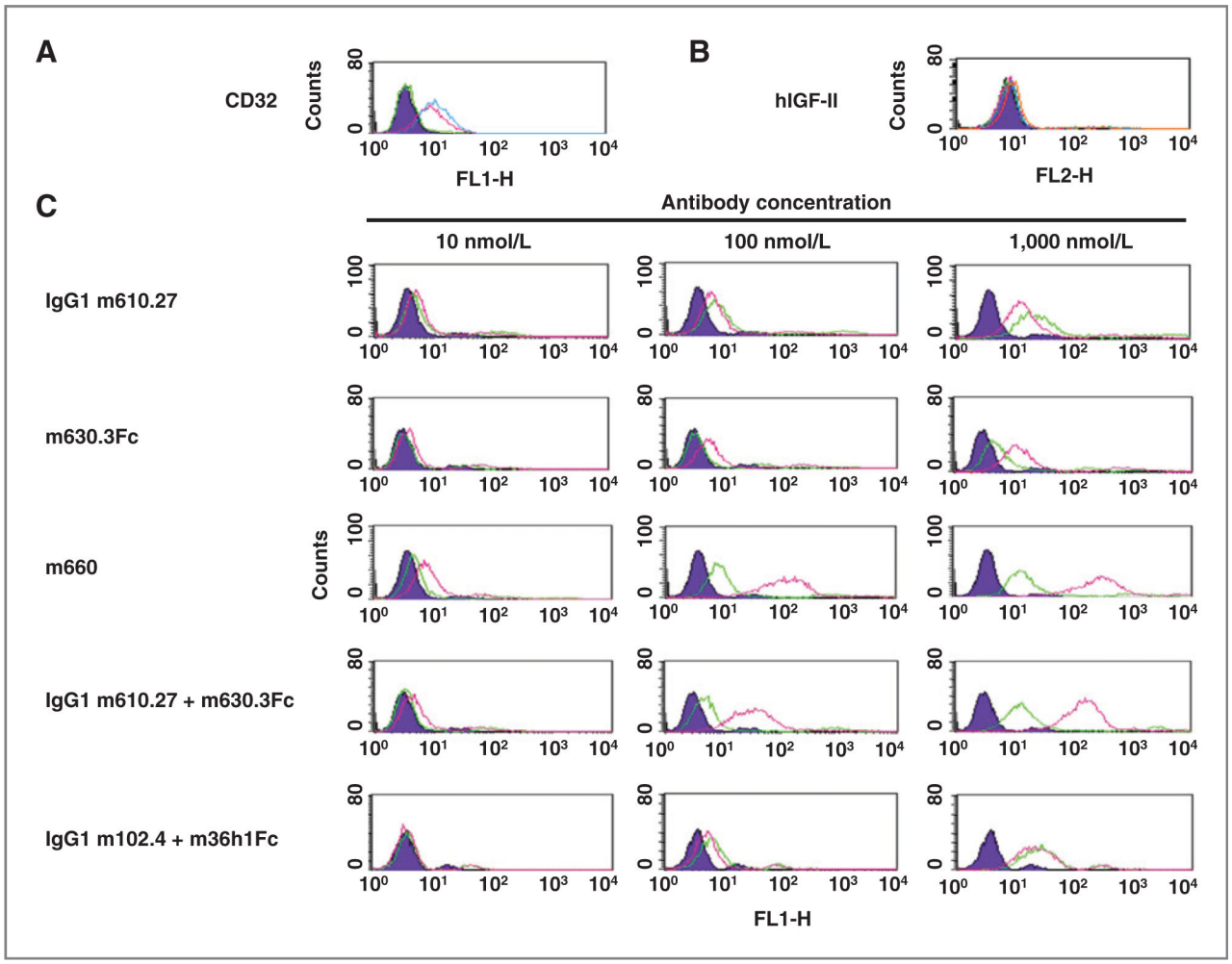

Figure 5.

FACS binding of antibody–hIGF-II complexes to BJAB cells. A, expression of FcγRII on BJAB cells. The diagram for reference cells is in purple. The diagram for cells incubated with 1:100 (v/v) diluted FITC-conjugated mouse anti-human CD16 (FcγRIII) antibody is in green. The pink diagram is for cells incubated with the anti-human CD32 (FcγRII) antibody at the same dilution. B, binding of biotinylated hIGF-II to BJAB cells. The green diagram indicates the cells incubated with streptavidin-PE conjugate only. The diagrams for cells incubated with hIGF-II at concentrations of 10, 100, and 1,000 nmol/L are in pink, blue, and orange, respectively. C, interactions of antibody–hIGF-II complexes with BJAB cells. The diagrams for reference cells are in purple. The green diagrams are for cells incubated with antibody alone. The pink diagrams are for cells incubated with a mixture of antibody and hIGF-II at a molar ratio of 1:2 (for monospecific antibodies) or 1:4 (for m660).

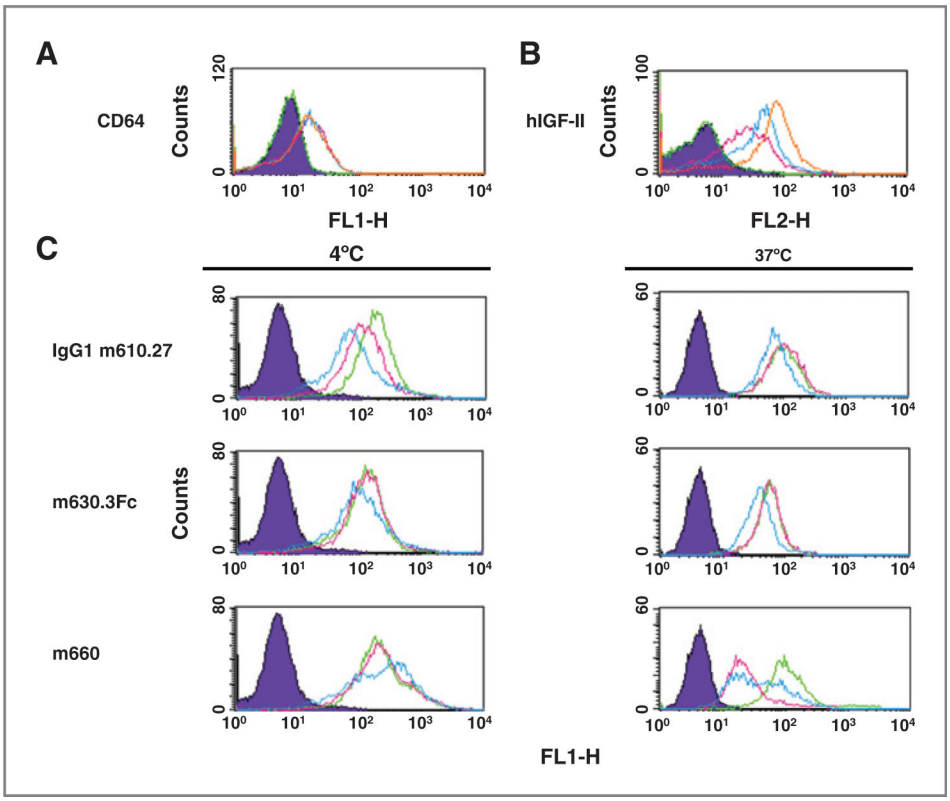

Figure 6.

FACS binding of m660–hIGF-II complexes to PMA-stimulated U937 cells. A, expression of FcγRI on U937 cells. The diagram for reference cells that were not stimulated is in purple. The diagram for cells mock-stimulated with PMA solvent dimethyl sulfoxide (DMSO) is in green. The pink, blue, and orange diagrams are for cells stimulated with 10, 20, and 30 ng/mL PMA, respectively. B, binding of biotinylated hIGF-II to U937 cells. The green diagram indicates cells incubated with streptavidin-PE conjugate only. The diagrams for cells incubated with hIGF-II at concentrations of 10, 100, and 1,000 nmol/L are in pink, blue, and orange, respectively. C, interactions of antibody–hIGF-II complexes with U937 cells. The purple diagram is for reference cells incubated with the secondary antibody only. The diagrams for cells incubated with 10 nmol/L antibody alone, 10 nmol/L antibody plus 20 (for monospecific antibodies), or 40 nmol/L (for m660) hIGF-II, and an combination of the antibody, hIGF-II, and 50 μmol/L cytochalasin D are in green, pink, and blue, respectively.